Impacts of Radio Frequency Interference in Synthetic Aperture Radar Data

Mingliang Tao*, Jia Su
Research & Development Institute of Northwestern Polytechnical University in Shenzhen
School of Electronics and Information, Northwestern Polytechnical University, 710072 Xi'an, China

Abstract

Synthetic aperture radar (SAR) is a very important instrument for active remote sensing. However, it is common to find that SAR echoes are often contaminated by electromagnetic interference, which is referred to as radio frequency interference (RFI). This paper analyze the impact of interference on SAR image and its post products. Qualitative and quantitative analysis of the adverse impacts of RFI on the simulated are illustrated from two perspectives, i.e., evaluation of imaging quality and interpretation of scattering mechanisms.

1. Introduction

For those high-resolution synthetic aperture radar (SAR) systems with large bandwidth, it is unavoidable to share spectrum with other services. It is common to find the SAR echoes are contaminated by the radio frequency interference (RFI), especially in low-frequency band [1]-[2]. RFI may come from external electromagnetic devices which share overlapping spectrum with the SAR systems, i.e., radiolocation radars, telecommunication devices, television networks, etc. [1]-[2]. The existences of RFI pose a hindrance to SAR image formation and image interpretation [3]. In order to improve the robustness of a SAR system in congested electromagnetic environments, it is of great importance to analyze the effects of interferences on SAR data. The goal of this paper is to reveal the relationship between RFI and polarization, as well as to analyze the impact of interference on SAR image and post products. Research on effects of RFI can help identify the weakness of current SAR systems, which could provide feedback for subsequent research on interference mitigation and system development.

2. Signal Model

Figure 1 shows the geometry of an airborne SAR system. The projection of the radar platform at slow time $t_m = 0$ on the ground is assumed to be the origin of Cartesian coordinates O-XYZ. $\hat{t}$ denotes the fast time along the range dimension. The X-axis denotes the azimuth direction and is set parallel to the radar ideal trajectory. The instantaneous coordinates of SAR system is

$\left[vt_m, y_S(t_m), H(t_m) \right]$, where $H(t_m)$ is the time-varying altitude of the SAR. $P(x_P, y_P, z_P)$ is a point target in the illuminated area, and $I(x_I, y_I, z_I)$ is a RFI emitter that behaves as an interference source to the SAR, whose spectrum overlaps with that of the SAR.
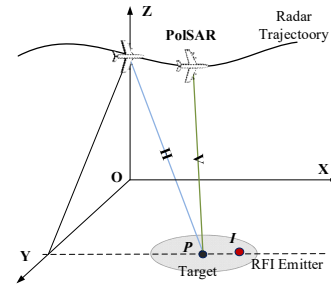

Figure 1. Geometry of a SAR system.

The voltage measured by SAR is related with the polarization state of radar receiver and the transmitter, which could be expressed as

$$V_{pq} = \left(h_p^{rec} \right)^T \cdot \mathbf{S} \cdot h_q^{tr} = \left(h_p^{rec} \right)^T \cdot \begin{bmatrix} S_{pp} & S_{pq} \\ S_{qp} & S_{qq} \end{bmatrix} \cdot h_q^{tr} \qquad (1)$$

where V_{pq} denotes the backscattering coefficient under the q-transmit p-receive polarization mode. $\mathbf{S}$ is the scattering matrix of the target. h^{rec} and h^{tr} denotes the Jones vectors which describe the polarization state of the radar antenna in receive and transmit mode, respectively.

Assume the SAR emits the signal $A(\hat{t})$. At time t_m, the radar echoes of point P under p-transmit and q-receive polarization states are expressed as

$$X_{qp}(\hat{t}, t_m) = \left(\left(h_q^{rec} \right)^T \cdot \mathbf{S} \cdot h_p^{tr} \right) \cdot A(\hat{t} - \Delta T_P) \exp(-j2\pi f_C \Delta T_P) \qquad (2)$$

where $\Delta T_P = 2R_P(t_m)/C$ denotes the two-way propagation delay of point target P. $R_P(t_m) = \sqrt{(vt_m - x_P)^2 + (y_S(t_m) - y_P)^2 + (H(t_m) - z_P)^2}$ denotes the instantaneous slant range from the radar to the point P. C is speed of light, and f_C denotes the carrier frequency. Similarly for the RFI emitter, assume it emits the time-varying signal $J(\hat{t})$, and thus the interference could be modeled as

$$I_{qp}\left(\hat{t},t_m\right)=\left(\left(h_q^{rec}\right)^T h^I\right)J\left(\hat{t}-\Delta T_I\right)\exp\left(-j2\pi f_C\Delta T_I\right) \quad (3)$$

where $\Delta T_I = R_I(t_m)/C$ denotes the one-way propagation delay from the RFI emitter I. $R_I(t_m)=\sqrt{(vt_m-x_I)^2+(y_S(t_m)-y_I)^2+(H(t_m)-z_I)^2}$ denotes the instantaneous slant range from the radar to the RFI emitter I at t_m. h^I is the transmitting Jones vector of the RFI emitter.

Therefore, for a specific polarization channel, the radar echoes could be expressed as a mixture of target echoes, interference from the RFI emitter and system noise,

$$D_{qp}\left(\hat{t},t_m\right)=X_{qp}\left(\hat{t},t_m\right)+I_{qp}\left(\hat{t},t_m\right)+N_{qp}\left(\hat{t},t_m\right) \quad (4)$$

where $N_{qp}\left(\hat{t},t_m\right)$ denotes the system additive noise.

3. Impacts of Radio Frequency Interference in Synthetic Aperture Radar Data

3.1 Impacts of Influences on Image Quality

In terms of the SAR raw data, the direct adverse impact of RFI is the reduction of signal-to-interference-plus-noise power ratio, especially with the presence of strong interference. Very strong RFI emissions could even saturate the receiver. It is not easy to identify the RFI in the time domain because of its additive nature with target echoes. However, RFI may appear well distinguishable in the range-frequency domain because of its relative narrow bandwidth compared to that of the radar echoes.

In case of motion compensation for high-quality SAR image formation, if some critical Doppler parameters (e.g., centroid and modulation rate) need to be estimated from the data, the presence of RFI would yield biased and inaccurate estimates, which would result in blurry and defocusing image or ghosts in the image. Figure 2 illustrates this phenomenon by using a real measured dataset in China, in which shows the estimate of azimuth Doppler rate in the case with and without RFI.
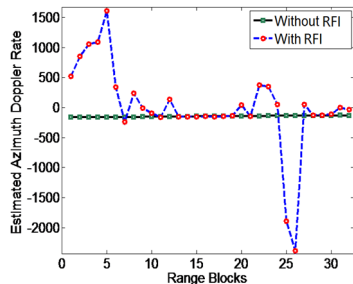

Figure 2. Variation of the estimated azimuth Doppler rate with range blocks in the case with and without interference effect.

The image formation process could be considered as a process of two-dimensional convolution of the raw echoes with a matched filter kernel in both range and azimuth direction, and expressed as

$$\sigma_{qp}\left(\hat{t},t_m\right)=D_{qp}\left(\hat{t},t_m\right)\oplus G\left(\hat{t},t_m\right)$$
$$=X_{qp}^G\left(\hat{t},t_m\right)+I_{qp}^G\left(\hat{t},t_m\right)+N_{qp}^G\left(\hat{t},t_m\right) \quad (5)$$

where σ_{qp} denotes the imaging result, $G\left(\hat{t},t_m\right)$ is the system response function of SAR imaging algorithm. $\oplus$ denotes the two-dimensional convolution operator. $X_{qp}^G\left(\hat{t},t_m\right)$ is equivalent to the imaging result of useful target echoes, which reflects the reflectivity. $I_{qp}^G\left(\hat{t},t_m\right)$ and $N_{qp}^G\left(\hat{t},t_m\right)$ denotes the output of RFI and noise after processing by the image formation step. According to (5), it is shown that the RFI is still mixed with the target echoes in a linear additive nature.

Owing to the 2-D matched filtering processing, SAR possesses a large signal processing gain along the range and azimuth, which endows it the inherent capability for interference suppression. It is worth noting that the matched filter is adapted to the target response and not to the RFI and noise. In terms of the focused imaging result, the large-power RFI will still superimpose on the focused image as visible artifacts or stripes, which may bury the target of interest and cause image quality degradation. The image quality can be evaluated by extracting the image response of a prominent point. The peak-to-sidelobe ratio (PSLR), integrated sidelobe ratio (ISLR) and impulse response width (IRW) along both the range and azimuth directions could be used as good metrics for image quality assessment. For distributed scene target, the effective number of looks (ENL) is a good candidate for evaluating the variation of noise level in the image due to the presence of interference. For RFI with weak power, it may not be obvious in the amplitude distortion, but may still have strong influence in phase distortion. Incorrect phase would lead to miscalculation of decomposition parameters, and inaccurate interpretation of scattering mechanisms. These will be discussed in next section.

3.2 Influences on Interpretation of Scattering Mechanism

The ultimate goal of PolSAR imaging is to obtain good understanding and interpretation of the illuminated area. Land-use classification is one of the most important applications of PolSAR. A kind of classification methods is based on the recognition of scattering mechanism between the electromagnetic waves and the medium. Van Zyl *et al.* first introduced the co-polarization and cross-polarization signatures as a useful tool for establishing the link with canonical scattering mechanisms [4].

Knowing the target response in a certain polarization basis, one can synthesize the radar cross section for any arbitrary combination of transmit and receive polarizations with a simple mathematical transformation. Hence, the synthesized 3-D co-polarized signature and cross-polarized signature are expressed as

$$P_{CO} = \left| \left(\mathbf{U} h_p^{rec} \right)^T \cdot \boldsymbol{\sigma} \cdot \left(\mathbf{U} h_p^{tr} \right) \right|^2 = \left| \left(\mathbf{U} h_p^{rec} \right)^T \cdot \left(\mathbf{X}^G + \mathbf{I}^G + \mathbf{N}^G \right) \cdot \left(\mathbf{U} h_p^{tr} \right) \right|^2 \quad (6)$$

$$P_X = \left| \left(\mathbf{U} h_q^{rec} \right)^T \cdot \boldsymbol{\sigma} \cdot \left(\mathbf{U} h_p^{tr} \right) \right|^2 = \left| \left(\mathbf{U} h_q^{rec} \right)^T \cdot \left(\mathbf{X}^G + \mathbf{I}^G + \mathbf{N}^G \right) \cdot \left(\mathbf{U} h_p^{tr} \right) \right|^2 \quad (7)$$

where $\mathbf{U}$ is the transformation matrix. τ is the tilt angle and ϕ is the ellipticity angle of the polarization ellipse characterizing the polarization state.

From (6)-(7), it is shown that the presence of interference would alter the shape and intensity of polarization signatures. Incorrect polarization signature may lead to misunderstanding of the scattering mechanisms, which would result in wrong classification results [5]. Besides, it will also cause error when using the polarization signatures to seek for the optimal polarization combination. To quantitatively evaluate the influence of interference, two metrics are introduced to compare the similarity between the polarization signatures without RFI and that with RFI, that is, the normalized signature correlation mapper (NSCM) measures the dissimilarity of the signature shapes, and the Euclidean Distance (ED) is used to compare the difference between the intensity of signatures [5].

3. Experimental Results

First, a simulation of point scatterers is provided for intuitive illustration. The radar is operated at L-band with fully linear-polarization capability. The radar system parameters are listed in TABLE I, which are set according to the National Aeronautics and Space Administration (NASA)/Jet Propulsion Laboratory (JPL) UAVSAR with minor modifications.

TABLE I. SYSTEM PARAMETERS FOR SIMULATION

Parameter Name	Value	Parameter Name	Value
Carrier Frequency	1.25 GHz	Platform Altitude	9 km
Pulse Duration	40 μs	Reference Slant Range	13 km
Bandwidth	150 MHz	Range Scene Extent	80 m
Azimuth Antenna Length	2 m	Azimuth Scene Extent	80 m
Pulse Repetition Frequency	400 Hz	Platform Velocity	150 m/s
Squint angle	$0°$	Polarization Mode	HH, HV, VH, VV

In the simulation scene, there are 13 scatterers marked by asterisk "*" as shown in **Figure 3**(a). An RFI emitter marked by cross "+" is located at (10m, 10m) which transmits time-varying chirp modulated wide-band interference. The transmitting polarization of the RFI emitter is assumed to be $^{+45°}$ linear polarized with a Jones vector of $\left[1/\sqrt{2} \quad 1/\sqrt{2} \right]^T$. The scatterers P1-P5 represent several canonical scattering mechanisms with polarization-varying backscattering coefficients. P6-P13 are identical scatterers with constant polarization-

invariant backscattering coefficients. The scattering matrices of the scatterers are illustrated in **Figure 3**(b).
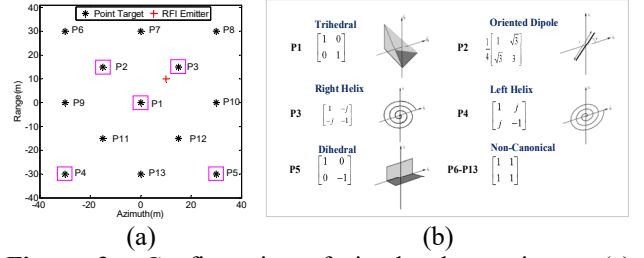

(a)   (b)

Figure 3. Configuration of simulated experiment. (a) Distribution of point scatterers. (b) Scattering matrices of the point scatterers.

3.1 Impacts on Image Quality

Figure 4 shows the imaging results with the presence of RFI under different interference-to-signal ratio (ISR). Thanks to the 2-D matched filtering process, SAR has inherent interference mitigation capability because of the large processing gain. After the non-coherent processing, the energy of interference spreads onto the whole image plane and behaves as noise. From Figure 4(b)-(d), it is shown that the noise floor of the image rises with further increase of ISR. Especially in Figure 4(d), the presence of interference submerges the image response of point scatterers, making it difficult to be detected. The presence of strong RFI would introduce significant distortions to the amplitude and phase of the image. Since the transmitting polarization of the RFI emitter is not orthogonal to that of the receive channel, all of the polarimetric channels are distorted by the presence of RFI. Without loss of generality, take the scatterer P2 for illustration. Its sectional drawings along the range and azimuth are illustrated in Figure 5.
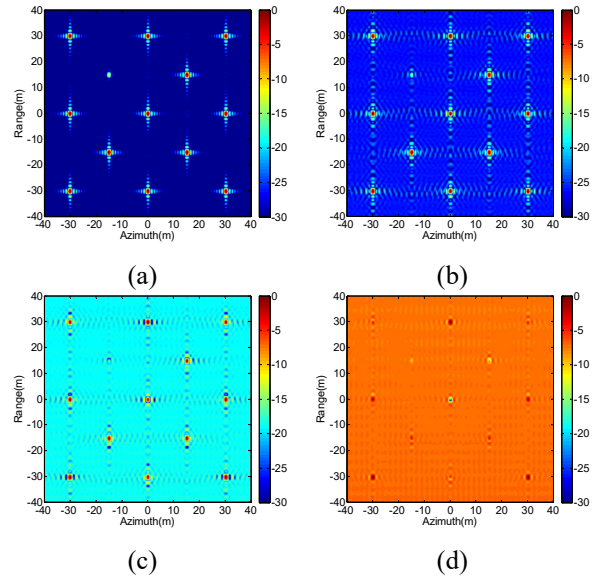

(a)   (b)

(c)   (d)

Figure 4. Imaging results of simulated SAR image with RFI under different ISR. (a) No RFI. (b) 26.61dB. (c) 34.57dB. (d) 50.13dB.
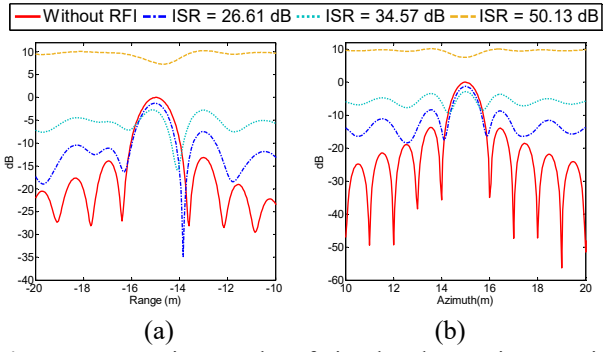
Figure 5. Imaging results of simulated SAR image with RFI under different ISR. (a) No RFI. (b) 26.61dB. (c) 34.57dB. (d) 50.13dB.

3.1 Impacts on Interpretation of Scattering Mechanism

One of the advantages of SAR is that it can provide abundant information of the medium and allows for the discrimination of different types of scattering mechanisms. The distorted amplitude and phase would alter the shape and intensity of polarization signatures. In this part, we will investigate the 3-D polarization signatures to have a better understanding of the RFI's effect on interpretation of scattering mechanisms.

To quantitatively evaluate the distortion, the normalized signature correlation mapper (NSCM) and Euclidean Distance (ED) are calculated. plots the variation of NSCM and ED with ISR. The NSCM measures the similarity between the shapes of signatures, and the ED reflects the difference between the intensity of signatures. For both the co-polarized and cross-polarized signature, the NSCM and ED are not sensitive to the interference in the beginning. With further increase of interference power, the NSCM and ED undergo sharp change. The significant distortion to the polarimetric signatures would pose a hindrance for the interpretation of the scattering mechanisms, and would definitely affect the performance of physical scattering characteristics-based classification scheme for SAR data.
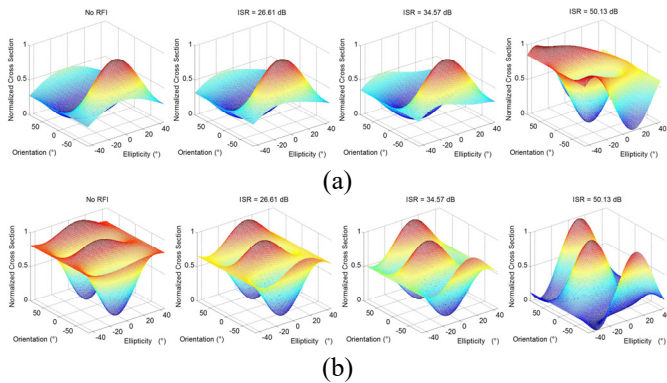

Figure 6. Co-polarized (a) and cross-polarized (b) signatures of point scatterer P2.
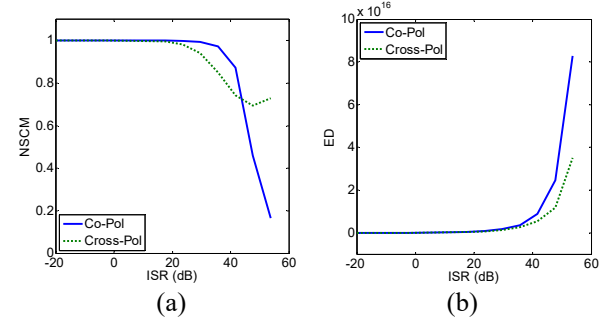

Figure 7. Evaluation of the distortion to the polarimetric signature of point scatterer P2. (a) NSCM. (b) ED.

5. Conclusion

The existences of RFI pose a hindrance to PolSAR image formation and image interpretation. This paper tries to establish the link between RFI and polarization, and mainly focuses on analyzing the effect of RFI on SAR image and its post products.

6. Acknowledgements

7. References

1. S. Misra, and P. Matthaeis, "Passive remote sensing and radio frequency interference (RFI): an overview of spectrum allocations and RFI management algorithms," *IEEE Geosci. Remote Sens. Mag.*, **2**, 2, June 2014, pp. 68-73, doi: 10.1109/MGRS.2014.2320879.

2. National Academies of Sciences, Engineering, and Medicine. *A Strategy for Active Remote Sensing Amid Increased Demand for Radio Spectrum*. Washington, DC: National Academies Press, 2015. doi: 10.17226/21729.

3. L. H. Nguyen and T. D. Tran, "A comprehensive performance comparison of RFI mitigation techniques for UWB radar signals," in Proc. of ICASSP 2017, 3086-3090.

4. Van Zyl J., and Y. Kim, Synthetic Aperture Radar Polarimetry, John Wiley and Sons, New Jersey.

5. M. Jafari, Y. Maghsoudi, and M. J. Valadan Zoej, "A new method for land cover characterization and classification of polarimetric SAR data using polarimetric signatures," *IEEE J. Sel. Topics Appl. Earth Observ. Remote Sens.*, **8**, 7, July 2015, pp. 3595-3607, doi: 10.1109/JSTARS.2014.2387374.